JPE 3-4-4

Transient Performance of a Hybrid Electric Vehicle with Multiple Input DC-DC Converter

Maged N. F. Nashed

Electronics Research Institute, Cairo, Egypt

ABSTRACT

Electric vehicles (EV) demands for greater acceleration, performance and vehicle range in pure electric vehicles plus mandated requirements to further reduce emissions in hybrid electric vehicles (HEV) increase the appeal for combined on-board energy storage systems and generators And the power electronics plays an important role in providing an interface between fuel cells (FC) and loads This paper deals with a multiple input DC-DC power converter devoted to combine the power flowing of multi-source on energy systems. The multi-source is composed of (i) FC system as a prime power demands, (ii) super capacitor banks as energy storage devices for high and intense power demands, (iii) superconducting magnetic energy storage system (SMES), (iv) multiple input DC-DC power converter and (v) a three phase inverter-fed permanent magnet synchronous motor as a drive In this system, It is used super capacitor banks and superconducting magnetic energy replaces from the battery system. The modeling and transient performance simulation is effective for reducing transient influence caused by sudden charge of effective load The main purpose of power electronic converters is to convert the DC power output from the fuel cell and other to a suitable AC voltage, which can be connected to electric loads directly (PMSM) The fuel cell and other output is connected to the DC-DC converter, which regulates the DC link voltage

Keywords: Fuel Cell system, superconducting magnetic energy storage (SMES), multiple input DC-DC power converter ultracapacitor tank and FLC

1. Introduction

The fuel cell (FC) system is one of preferable power sources with high energy conversion efficiency, considering the environmental problems associated with energy consumption Considerable efforts have been expended to develop hybrid electric vehicles (HEVS) as replacements for high-emission cars, buses, and trucks powered by conventional gasoline or diesel engines[1]

The main objective of this paper is to describe a virtual prototype of a HEV by the use of a suitable simulation model This is an important step in the development of the HEVs due primarily to the reason a good virtual prototype allows for proof testing before hardware is assembled, which means likely reduction in the manufacturing cost and time The electrical part of the HEV considered in this study is composed of a fuel cell system as the prime source of average electric power (10 to 15 kW),

Superconducting magnetic energy and super capacitor banks as energy storage devices for start, high and intense power demands (e g., 50&150 kW, respectively),

---

Boost and bi-direction type DC-to-DC power converters to control the flow of power, DC current/ DC voltage converter to control the flow of SMES

A pulse-width modulated (PWM) inverter-fed three-phase permanent magnet synchronous motor (PMSM) with associated vector controller as a drive and A common DC bus for energy distribution

The HEV supply complex has excellent characteristics of high energy efficiency taking full advantage of the FC as well as SMES Furthermore, SMES enables the hybrid power source to compensate the transient shock in the utility system caused by the sudden change of the effective and reactive load demands It is the purpose of this paper to propose a highly efficient FC system that is very co-operative with the existing utility system[2][3]

2. System Configuration

Fig 1 shows a simplified block diagram for the electrical part of the HEV As well known, the FC system is a very preferable power system from the viewpoint of environmental consideration, and SMES is an excellent energy storage system, which has high energy efficiency and sufficient response time in combination with advanced power electronics converters[2].

SMES is also expected to withstand charge/discharge operations of many cycles, as compared with lead acid storage battery The output of SMES is converted from dc current mode to dc voltage mode by the current/voltage converter The current/ voltage converter has a function to keep the output voltage at a constant value This means the dc chopper (DC/DC converter) is operated at the given output voltage The output power of FC can be controlled by adjusting the input voltage of DC/DC converter Additional filters may be used to improve the quality DC-AC inverter is connected to the DC link and converts the DC voltage to AC The control of the inverter is generally achieved by PWM techniques[4] Explanations of the models are given in the next section Based on the component descriptions, a virtual prototype of the HEV is then built The definitions of the fuel cell system, SMES, super capacitor bank, boost converter, bi-direction converter, DC current/ DC voltage, PMSM, and the PWM inverter are given in the following subsections Finally, simulation results are presented to numerically verify the virtual prototype.

2.1 Full Cell System

The voltage-current characteristic of a single PEM (proton exchange membrane) hydrogen fuel cell is illustrated in Fig. 2. In this figure, V_{fc} (vertical axis) is the voltage at the terminals of the fuel cell, P_{fc} (other vertical axis) is the power at the terminals of the fuel cell and I_{fc} (horizontal axis) is the current flowing out of the fuel cell It is seen that there are basically three operation regions These are, (i) the low current region in which the voltage decreases exponentially as the current increases, (ii) the linear region that covers a large portion of the characteristic, and (iii) the high current region in which there is a sharp drop of the voltage to near-zero[5].
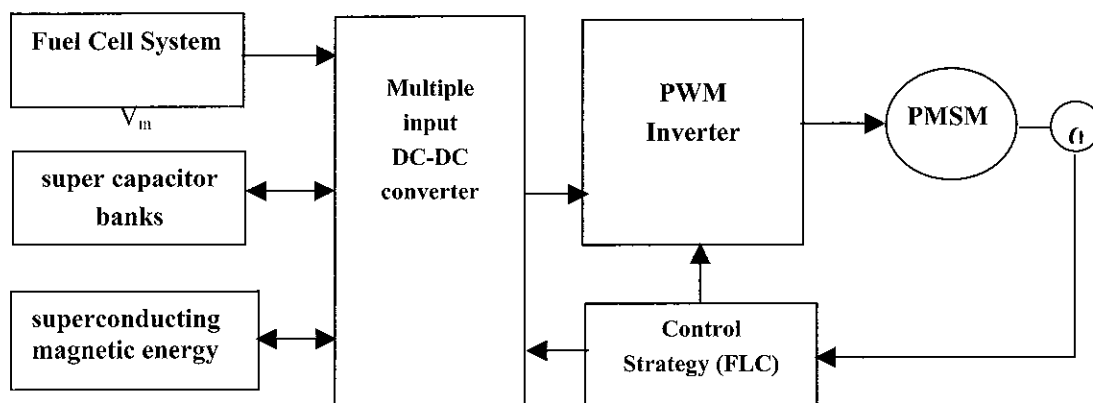

Fig 1   A simplified block diagram for the electrical part of the hybrid electric vehicles
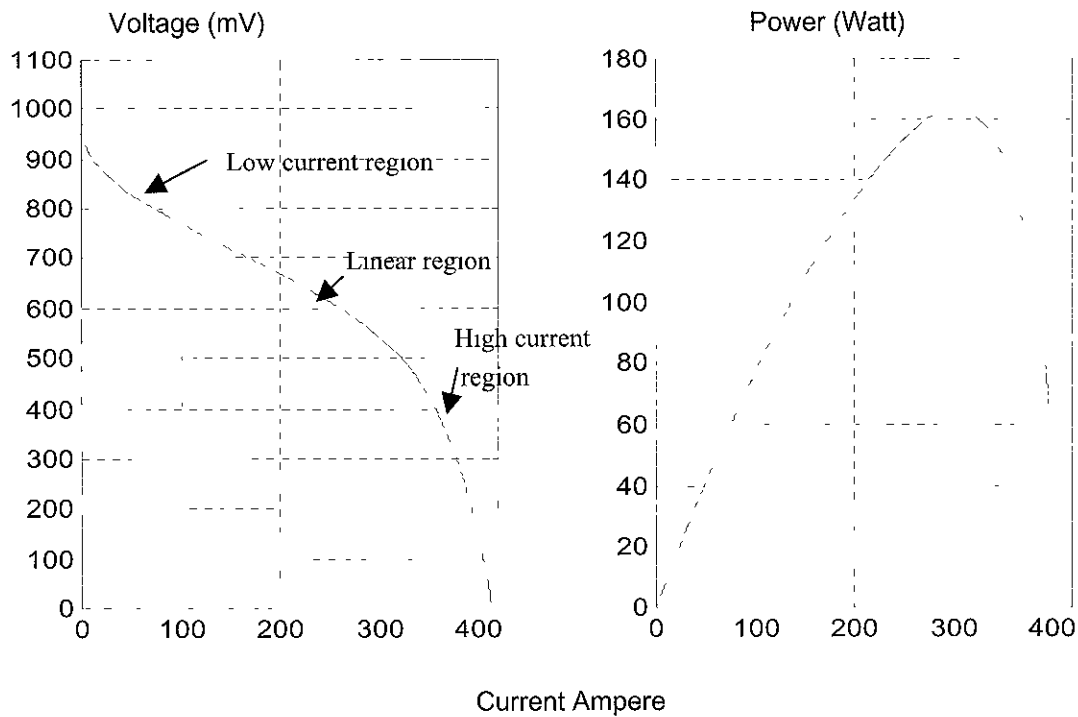
Fig 2   The fuel cell voltage in mV, power in watt versus fuel cell current in A

Note also that, the units for V_{FC} is millivolts

For the values of I_{fc} which remain in the low current and linear regions, V_{fc} versus I_{fc} may be expressed by

$$V_{fc} = V_{fc0} - b\log(I_{fc}/A_{fc}) - R_{fc}I_{fc} \qquad (1)$$

Where V_{fc0} is the open-circuit (zero current) voltage of the fuel cell in mV, b is the Tafel slope in mV, A_{fc} is the cross-sectional area of the fuel cell in cm^2, and R_{fc} is the internal ohmic resistance of the fuel cell in Ω[5]

The total voltage of a fuel cell stack is given by

$$V_{fctotal} = N_{fc}V_{fc} \qquad (2)$$

where, N_{fc}, is the number of cells in the stack

The numerical values for the fuel cell parameters are listed in appendix A

The fuel cell system under consideration produces power up to 18 kW This is enough to overcome average air drag and other losses at highway speeds Another consideration is that the output voltage of the fuel cell system is always low when compared with the common DC bus voltage This calls for an intermediate DC-to-DC power converter which is capable of transferring the energy from one side with lower voltage to another with higher voltage

2.2 Super Capacitor Bank and superconducting magnetic energy storage (SMES)

In this work, a single double-layer super capacitor is represented by the circuit in Fig 3, which consists of all equivalent series resistance R_{esi}, and an ideal capacitance C_{ideal} The equivalent series resistance accounts for the losses in the super capacitor[6]

As shown in Fig 3. let V_{super} and I_{super} denote, respectively, the voltage at the terminals of the super capacitor and current flowing into the super capacitor. The voltage-current relationship of the super capacitor is then expressed by

$$V_{super} = R_{esi}I_{super} + \frac{1}{C_{ideal}}\int_0^t I_{super}\,dt + V_{ideal}(0) \qquad (3)$$

where $V_{ideal}(0)$ is the initial voltage across the ideal capacitance C_{ideal} Note that $V_{super}(0)$ (the initial value of V_{super})is equal to $V_{ideal}(0)$ if $I_{super}(0)$ (the initial value of I_{super}) is zero
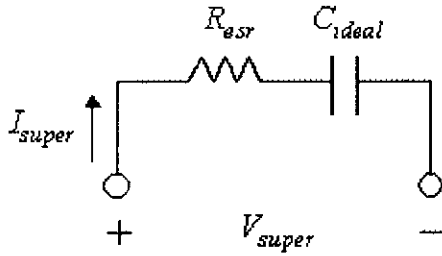
Fig 3   The equivalent circuit for the super capacitor

Appendix B lists the parameter ratings of single double-layer super capacitor[6].

To achieve higher voltage rating, the series and parallel connections of the super capacitors are considered in this work Specifically, a super capacitor network of 4 parallel branches is utilized, where each branch consists of series connections of 200 super capacitors This results in a super capacitor bank, the overall voltage rating, capacitance and series resistance of which are 460 V, 9 4 F and 0.225 Ω, respectively. The overall initial voltage of the super capacitor bank is set to 460 V in the simulation.

The super-capacitor bank contributes to the peak and intense power requirements of the HEV, which might be as high as 160 kW and as brief as few seconds This is necessary to accelerate the vehicle under consideration to a speed of 50 km/hr capacitor bank also accepts (transiently) part of the energy released by the drive motor during regenerative braking[7]

The voltage across the super capacitor bank might swing above and below the common DC bus voltage considerably due to the excessive incoming and outgoing currents during rapid braking and acceleration. This necessitates an intermediate bi-directional, DC-to-DC power converter, which is capable of operating in both up and down modes.

On the other hand SMES enables the hybrid power source to compensate the transient shock in the system caused by the sudden change of the effective and reactive load demands SMES is connected to the bus line through a bi-directional converter Assuming that the current flowing through SMES at the initial time of charging is I_o, the relationship between the required stored energy W and the charging period T is obtained as follows.

$$W = \frac{1}{2} L I_{SMES}^2 + \left| P_{SMES} \right| T \tag{4}$$

where L· is inductance of SMES

I_{SMES} Current value at the end of the charging period

Rewriting the above equation, we can obtain the current value I_{SMES} of SMES as a function of the charging time T

$$I_{SMES} = \sqrt{I_0^2 + \frac{2 \left| P_{SMES} \right| T}{L}} \tag{5}$$

From equation (4), capacity and discharge time of SMES are determined by equation (6).

$$\tau \Delta p = \frac{1}{2} L I_{SMES}^2 K \tag{6}$$

where:τ .is response delay time of FC

Δp Incremental portion of the effective power

K. Discharging rate of SMES

In order to evaluate the relation between capacity and discharge time of SMES, response delay time of FC τ is given by equation (7)

$$\tau = (\frac{1}{2} L I_{SMES}^2 K) / \Delta p = WK / \Delta p \tag{7}$$

2.3 Power Converters for Fuel Cell System and Super Capacitor

The fuel cell system and super capacitor are connected to the common DC power bus through DC-to-DC power converters of the step-up and bi-directional topologies. The converter associated with the fuel cell is step-up type and commands the energy transfer out of the fuel cell. Fig. 4 shows the circuit of the FC system and DC-DC converter. The operation of this circuit is as follows Resistance r is the lost energy consumption by internal resistance of FC corresponding to 30% loss. Inductor L_1, L_2 and capacitor C_2 have smoothing function for current and voltage respectively. In addition capacitor C_1 has DC snubber-less function When switch SW is closed, adjusting the output voltage of FC V_{fc} controls the output power of FC V_{fc} can be controlled by the duty cycle α can be varied from 0 to 1.

On the other hand, the converter for the super capacitor is bi-directional converter. It controls the power flow into and out of the super capacitor Fig 5 is the circuit diagram for the bi-directional converter
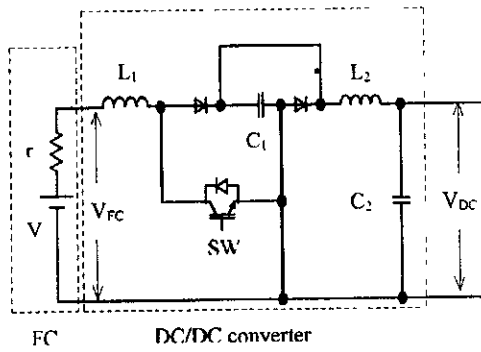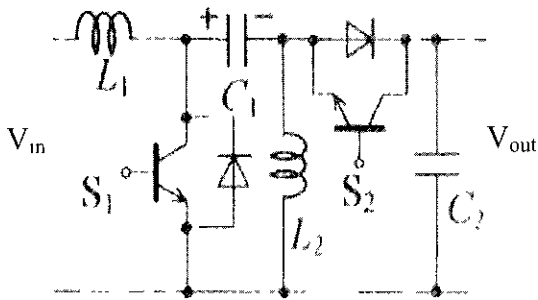
Fig 4   The circuit of the FC system and DC-DC converter

Fig 5   The circuit diagram for the bi-directional converter

The corresponding average model is·

$$\frac{di_{L_1}}{dt} = \frac{v_{in} - (1-D)v_c}{L_1} \tag{8}$$

$$\frac{di_{L_2}}{dt} = \frac{Dv_c - v_{out}}{L_2} \tag{9}$$

$$\frac{dv_c}{dt} = \frac{(1-D)i_{L_1} - Di_{L_2}}{C} \tag{10}$$

where D is duty ratio defined in a similar manner

And there is another converter The output of SMES is converted from DC current mode to DC voltage mode by the current/ voltage converter. The current/voltage converter has a function to keep the output voltage at a constant value Fig 6 shows the circuit of the I/V converter[2]. The operation of this circuit is as follows When the voltage of the capacitor (hereafter V_{SMES}) is below a set value, IGBTs are turned off, and the current of SMES (hereafter I_{SMES}) flows into the capacitor Consequently V_{SMES} rises. When V_{SMES} goes up above a set value, IGBT is turned on And I_{SMES} tends to circulate

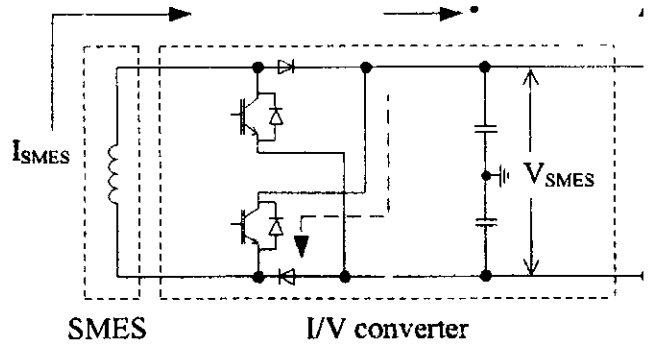SMES   I/V converter

Fig 6   The I/V converter circuit

in SMES in the steady state mode. V_{SMES} is kept constant repeating the above-mentioned operation

2.4 Three-Phase PMSM

The *d-q* model of the three-phase PMSM considered for the HEV is given by

$$\frac{dI_d}{dt} = \frac{V_d}{L} - \frac{R_s}{L}I_d + p\omega I_q \tag{11}$$

$$\frac{dI_q}{dt} = \frac{V_q}{L} - \frac{R_s}{L}I_q + p\omega I_d - \frac{3}{2}\frac{p}{L}\omega\lambda_{max} \tag{12}$$

$$\frac{d\omega}{dt} = \frac{1}{k_2}(T_e - k_0 - k_1\omega^2) \tag{13}$$

where V_d and V_q are the stator d and q voltages, I_d and I_q are the stator d and q currents, ω is the angular velocity of the rotor, R_s is the resistance of the stator phase winding, L is the inductance of the stator phase winding, p is the number of pole-pairs, and λ_{max} is the flux linkage due to the permanent magnets The parameters k_0, k_1 and k_2 are related to the force opposing the motion of the vehicle In equation (13), T_e is the electrical torque (that is, the torque produced by the motor) and is computed from

$$T_e = p\lambda_{max}I_q \tag{14}$$

The stator d-q voltages V_d and V_q are related to the stator three-phase voltages V_a, V_b, and V_c by

$$\begin{bmatrix} V_d \\ V_q \end{bmatrix} = \begin{bmatrix} \cos(p\theta) & \sin(p\theta) \\ -\sin(p\theta) & \cos(p\theta) \end{bmatrix} \begin{bmatrix} 3/2 & 0 & 0 \\ 0 & \sqrt{3}/2 & -\sqrt{3}/2 \end{bmatrix} \begin{bmatrix} V_a \\ V_b \\ V_c \end{bmatrix} \tag{15}$$

The same relationship is also valid for the stator d-q and three-phase currents The parameter values for the PMSM are listed in appendix

2.5 PWM Inverter for PMSM

Over the years, the space vector pulse-width modulation (SVPWM) technique for voltage source inverters has received widespread acceptance due to its implementation simplicity and superior performance characteristics such as low harmonic loss factor The linear modulation range of SVPWM technique terminates at a modulation index of $\sqrt{3}\pi/6 = 0.9073$ [4] In other words, with SVPWM scheme, the maximum value of the fundamental component of the output (phase) voltage that can be commanded without introducing low-order harmonics is $V_{dc}/\sqrt{3}$ where V_{dc} is the DC link (bus) voltage Taking this into account, the stator d-q voltages of the PMSM are limited by (see transformation equation (15))

$$\sqrt{V_d^2 + V_q^2} \leq \frac{\sqrt{3}}{2}V_{dc}$$ (16)

Assuming that the inverter is lossless, the input current I_{dc} into the inverter is calculated by setting $P_{in}=P_{out}$ and then solving for I_{dc} Where,

$$P_{in} = V_{dc}I_{dc}$$ (17)

is the input power to the inverter and

$$P_{out} = \frac{2}{3}(V_dI_d + V_qI_q)$$ (18)

is the output power delivered by the inverter to the PMSM[26] The expression for I_{dc}, is then obtained as,

$$I_{out} = \frac{2}{3}\frac{V_dI_d + V_qI_q}{V_{dc}}$$ (19)

The constraint (16) and expression (19) represent an average-value model for the SVPWM inverter

3. Control Strategy

Actually we begin by measuring the error between the

actual speed and the reference speed From this error and the change of error we can build a set of rules to control the speed. This controlled speed gives us a good indication about the volt which must applied to the motor. Fig 7 shows the block diagram of the system In this section, two blocks for FLC are explained The range of output variable is taken to match the range of root mean square value of the voltage, which gives the indication of what value of speed must be changed to reach the reference speed. To verify the control technique V/F= constant, the second stage of FLC is designed to make the control more accurate and to give the chance for making a loop for controlling the current. The output of the first blocks of FLC becomes directly one of the two inputs of the second stage blocks[8].

The Fuzzy membership functions (MS) for the first stage control are exhibited in Fig 8 The system uses five memberships for each variable. While, Fig 9 shows the MS of the second stage control (V/f control)

The control rules of the first stage are defined heuristically as following.

Table 1   The rules of the first stage

Δerror / Speed Error	hn	ln	ze	lp	hp
hn	ze	lp	lp	hp	hp
ln	ln	ze	lp	hp	hp
Ze	ln	Ze	ze	lp	lp
Lp	hn	ln	ln	ze	lp
hp	hn	hn	ln	ln	ze

The control rules of the second stage are defined heuristically as following.

Table 2   The rules of the second stage

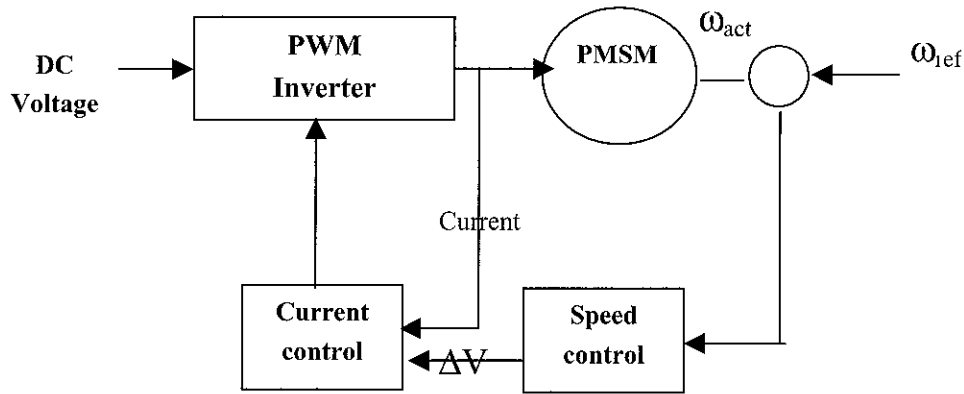| Volt / Current	hn	ln	ze	lp	hp
hn	ze	ln	ln	hn	hn
ln	lp	ze	ln	ln	hn
ze	lp	lp	ze	ln	ln
Lp	hp	lp	lp	ze	ln
hp	hp	hp	lp	lp	ze

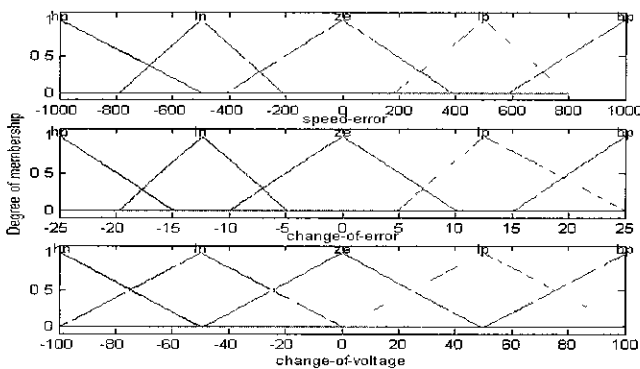Fig 7   Block diagram of the control system

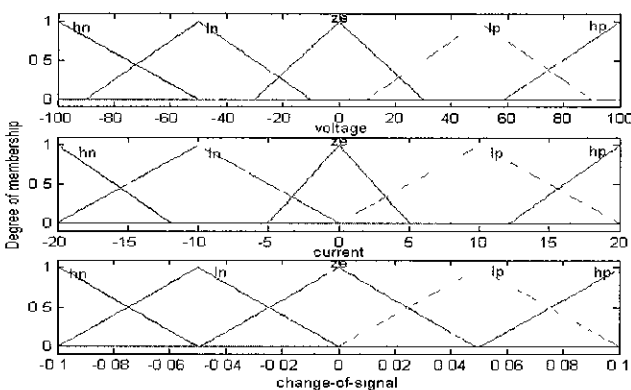Fig 8   Membership function of first stage

Fig 9   Membership function of second stage.

4. Simulation Results

The simulation of the proposed HEV system is carried for rapid acceleration and deceleration of driving cycles In this case, the vehicle was first accelerated to a speed of 14.5m/sec (52.2Km/hr.) in 7 seconds, then, constant keeps

the speed for 3 seconds, and finally, brings down to rest in 7 seconds Figs 10-14 show the results obtained with this move Fig. 10 displays the speed tracking performance of the vehicle In this figure, due to the close tracking, the actual and reference speeds are on top of each other

The input current I_{dc} into the PWM inverter and the DC bus voltage V_{dc} are given in Fig 11 It is seen that during the acce-leration phase (from 0 to 7 sec), V_{dc} drops as I_{dc} increases. On the other hand, in the deceleration phase (from 10 to 17 sec), V_{dc} reaches a peak value During the dece-leration, the energy supplied by the motor charges the SMES via the DC bus As a result, the DC bus voltage, which is floating at the SMES voltage, increases The Torque and speed motor are given in Fig 12.
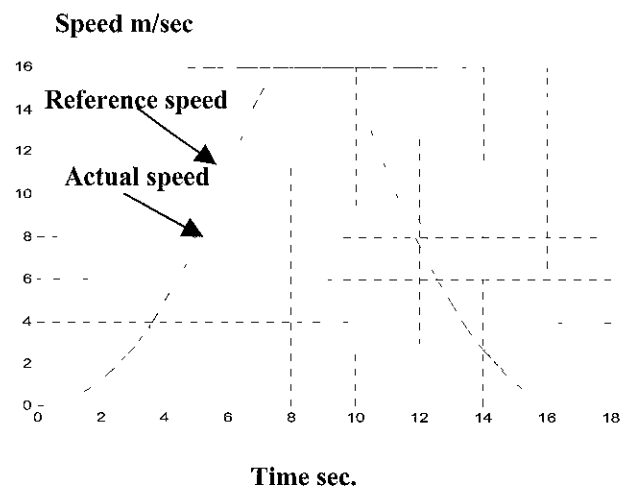

Fig 10   Actual and reference speeds of HEV (maximum speed 14 5 m/sec)
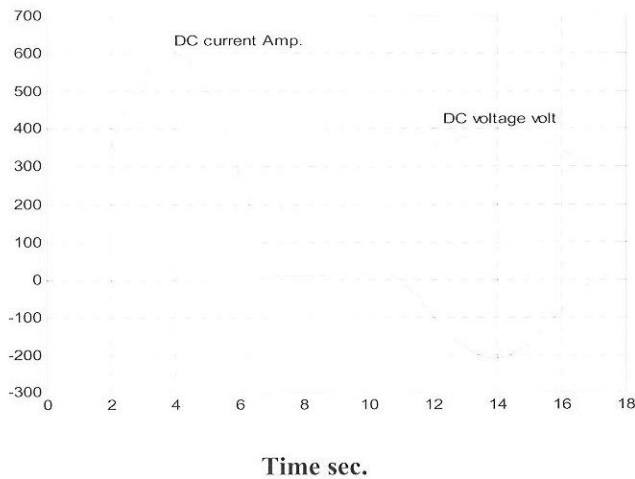
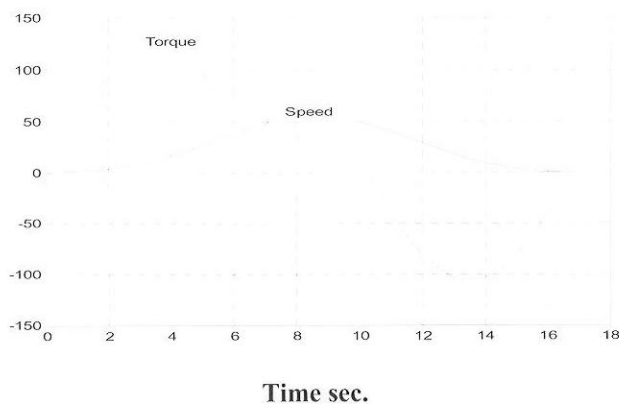**Fig. 11.** Input current in amperes and voltage in voltage to inverter.

Fig. 12. The motor torque in N/m and vehicle speed in km/hr.
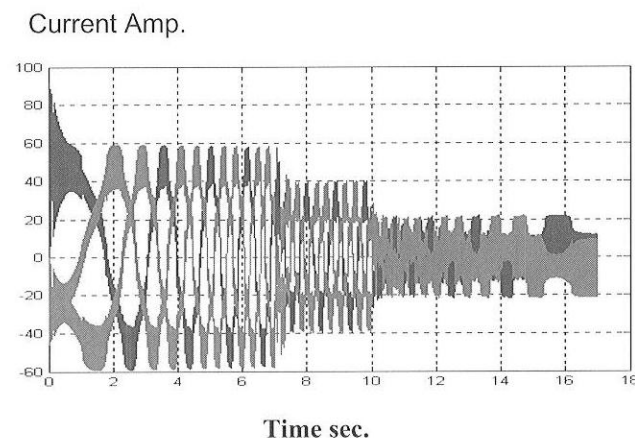
Current Amp.

Fig. 13. The three phases motor current in amp..

The three phases motor current are shown in Fig. 13. Fig. 14 shows the total input power P_{in} to the inverter and
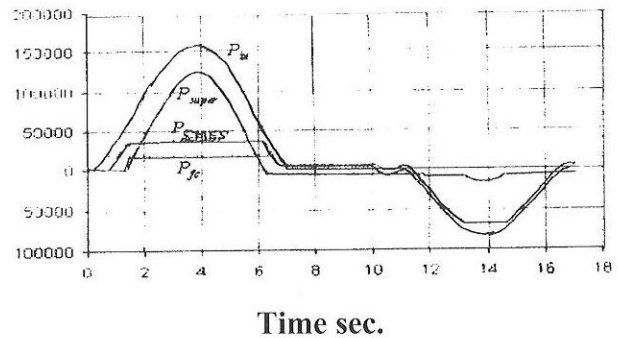

Fig. 14. Contribution of each energy device to the total input power.

contributions of the fuel cell P_{fc} , super capacitor P_{super} and SMES P_{SMES} to P_{in}. During the acceleration, the fuel cell system is commanded to provide power up to the 18 kW. On the other hand, the SMES system together with the fuel system provides just about 55kW (maximum). Finally, the super capacitor supplies the rest of P_{in}, which goes up to 160 kW during the acceleration.

5. Conclusions

A virtual prototype for a HEV was developed and also numerically verified by simulation results within the VTB environment. The virtual prototyping was achieved using the VTB native models of the components. Also, based on the simulation results, a full motion animation of the HEV was performed to demonstrate the advanced visualization capabilities of the VTB. The SMES system and super capacitor bank are effective to compensate the sudden change of the load demands.

One of the unique features of the virtual prototype is that it includes all possible energy devices (full cell system, SMES system and super capacitor bank) for the next generation HEVS. Further, to be consistent with the nonlinear dynamics, ohm losses, and voltage/current limits of the components are taken into account.

Appendix A

* Fuel cell parameters:
  V_{fco}=1000mV, b=25mV, A_{fc}=292cm^2,
  R_{fc}=0.000819Ω, m=0.0475mV, n=0.0065cm^2.mA^{-1},
  N_{fc}=110.

Appendix B

* Super capacitor:

C_{ideal}=470F, R_{esr}=4.5mΩ,

Rated voltage 2.3V, Max. current=343A.

* SMES:

Stored energy=10MJ, L=5H, I =2000A

* PMSM:

P=18KW, R_s=0.39Ω, L=0.444mH,

p=3, λ_{max}=0.0737Wb, J_m=0.0355kgm^2.

References

[1]   T. Aoki, Y. Ogami, and H. Nishikawa, "History of PAFC FC Performance Degradation Mode", Trans. IEE of Japan, Vol. 119-B, No. 4, pp. 500-506, April 1999.

[2]   R. Nojima and Y. Sawada, "Investigation on New Type Hybrid Dispersed Electrical Energy System with FC and SMES", National Convention Record, IEE of Japan, No. 6-139, pp. 2463-2464, March 2001.

[3]   M.J. Riezenman, "Engineering the EV future", IEEE Spectrum, vol. 35, No. 11, pp. 18-20, November 1998.

[4]   J. Holtz, "Pulsewidth modulation for electronic power conversion", Proceedings of IEEE, vol. 82, No. 8, pp. 1194-1214, Aug. 1994.

[5]   L.J. M.J. Blomen and M.N. Mugerwa, "Fuel Cell Systems", Plenum Press, New York, 1993.

[6]   R.L. Spyker and R.M. Nelms, "Evaluation of double layer capacitor technologies for high power and high energy storage applications", Pro. of 23rd Inter. Conf. on Industrial Electronics, Control, & Instrumentation, ICON '97, New Orleans, Louisiana, pp. 1086-1091, Nov. 1997.

[7]   L.U. Gokdere, C.W. Brice, and R.A. Dougal, "Hybrid electric vehicle with permanent magnet traction motor: A simulation model", Proceeding of IEEE Inter. Electric Machines and Drives Conference, IEMDC '99, Seattle, Washington, pp. 502-504, May 1999.

[8]   C.C. Lee, "FLC Systems, I and II", IEEE Trans. System Man, Cybern, Vol. 20, pp. 404-435, April, 1990.

Maged Naguib Fahmy Nashed was born in Cairo, Egypt, in 1962. He eceived B. S. degrees in Electrical Engineering, from the univ of Menoufia University, Egypt, in May 1983, the Diploma of Higher, from Cairo Univ., May 1990, the M.Sc degree in Electrical Engineering, from Ain shams univ., Cairo, Egypt, in April 1995 and the Ph. D. of degree in Electrical Engineering, from Ain shams Univ., Cairo, Egypt, in January 2001. Since 1989, he has been with the Dept. of Electronic and Energy conversion. Electronic Research Institute, where he is currently a Researcher. He is engaged in research on Power Electronic, Drive circuit, control of drives and Renewable Energy.